

CHARACTERISTICS AND MAGNETIC PROPERTIES OF ((80-x) P₂O₅: 20 SiO₂: x Al₂O₃) AND DOPED WITH Ni₂O₃ PREPARED BY SOL GEL METHOD

A. M. EL-NAHRAWY^{a*}, M. M. ELOKR^b, F. METAWE^c, B. A. A. OSMAN^d

^a*Department of Solid State Physics, National Research Centre (NRC)-33*

ElBohouth st., P.O.12622, Dokki, Giza, Egypt.

^b*Physics Department, Faculty of Science, Al Azhar University, Nasr City, 11884 Cairo, Egypt.*

^c*Department of Mathematical and Physical Engineering, Shoubra Faculty of Engineering*

Benha University, Egypt.

^d*Department of Basic Engineering Sciences, Benha Faculty of Engineering, Benha University, Egypt.*

phosphosilicate (80 P₂O₅: 20 SiO₂) nanoparticles modified with three different concentrations of Al₂O₃ ions (10, 15, 20 mol %) and doped with Ni₂O₃ in the formula (59 P₂O₅: 20 SiO₂: 20 Al₂O₃: 1 Ni₂O₃) were prepared by sol-gel method at room temperature using triethylphosphate, tetraethylorthosilicate, aluminum and nickel nitrates as a sources for P₂O₅, SiO₂, Al₂O₃ and Ni₂O₃. Monolithic, transparent gels were formed with both prepared samples and calcined at 900°C for 3h in air. The effect of Al₂O₃ contents on the morphological properties of pure and doped phosphosilicate were investigated. The prepared monolithic samples were characterized by X-ray diffraction (XRD), transmission and scanning electron microscopy (TEM/SEM), Fourier transform infrared spectroscopy (FTIR). X-ray diffraction and FT-IR showed that the addition of Al₂O₃ caused the formation of phosphosilicate network as P–O–Si, and formation of aluminophosphosilicate network as P–O–Si–O–Al. The magnetite measurement is formed for the aluminophosphosilicate system doped with 1 mol% Ni₂O₃ ions, using the vibrating sample magnetometer (VSM) at room temperature.

(Received June 16, 2016; Accepted October 1, 2016)

Keywords Sol gel processes, phosphosilicate glass, aluminophosphosilicate nanoparticles, XRD, FTIR, VEM.

1. Introduction

Recently, phosphosilicate-based glasses have attracted considerable attention because of their capability to use in multi-applications as optical, electronic, bioglasses due to bioactivity and biocompatibility [1-4]. The phosphosilicate-based glasses have unusually low characteristic temperatures less than required for single phosphate or silicate glasses. Also, increasing interest has been devoted to sol gel phosphosilicate materials because of a chemical composition, ability to introduce high concentrations of transition metal ions and chemical stability [5, 6]. Sol gel phosphosilicate glass-ceramics are polycrystalline materials obtained by controlled crystallization of parent glasses [6, 7]. Depending upon the composition source of the parent glasses and the calcination temperature, various properties of the glass and glass-ceramic and dopents level can be precisely controlled [7-9]. These modified phosphosilicate glasses are technologically and industrial important because of their excellent optical properties and chemical durability and are widely used in various applications [7, 10]. Addition of different modifiers as transition metals ions (M), where (M= Ni, Co, Fe, Al, Mn, Cu) to phosphosilicate glasses results in lowering the calcination temperature, open structure, tetrahedral structural units. The metal ions were embedded

*Corresponding author: amany_physics_1980@yahoo.com

during the preparation sol gel process at room temperature. The addition of Al_2O_3 and different transition elements to phosphosilicate glasses is well-known to improve the chemical durability and stability and affect other properties [11, 12]. At higher Al_2O_3 content AlO_3 groups are formed as well. The oxygen from the metal oxide as modifiers for the phosphosilicate glasses becomes part of the covalent network creating new structural units (P–O–Si, P–O–Al, Si–O–Al, Si–O–Al–O–Ni and P–O–Si–O–Al). The sol–gel process is attractive chemical method because it offers precise control of composition, high purity and homogeneity, easy processability, low cost and offers large-surface area systems [11-14]. Sol–gel method is an effective and simple technique to prepare inorganic, organic and organic/inorganic materials in different forms such as nano-wires nano-rods, monolithic, membranes, films and ceramics. In the present work, we have studied the incorporation of Al_2O_3 ions into phosphosilicate glasses. It's known that phosphate glasses reveal a low chemical durability, we have chosen as a base glass the composition (80 P_2O_5 : 20 SiO_2) because the replacement of 20 mol% P_2O_5 by SiO_2 and another (10-20 mol %) results in a glass with better physicochemical properties. The produced powders were characterized by X-ray diffraction (XRD), transmission and scanning electron microscopy (TEM/SEM) and Fourier transformed infrared (FTIR) spectroscopy. The relations between structural changes and the changes in physicochemical properties will be discussed as well. The magnetic properties for the prepared samples were investigated.

2. Experimental work

Pure phosphosilicate (80 P_2O_5 : 20 SiO_2) modified with three different concentrations of Al_2O_3 ions, ((80-x) P_2O_5 : 20 SiO_2 : (x=10, 15, 20) Al_2O_3) (based on mol %) and (59 P_2O_5 : 20 SiO_2 : 20 Al_2O_3 : 1 Ni_2O_3) nanoparticles were prepared by a sol–gel process. First, pure monolithic phosphosilicate were obtained by hydrolysis and condensation of triethylphosphate (TEP) ($\text{C}_2\text{H}_5\text{O})_3\text{P}(\text{O})$ as P_2O_5 , tetraethoxysilane ($\text{C}_2\text{H}_5\text{O})_4\text{Si}$ (TEOS, 99.999%, Sigma-Aldrich) as SiO_2 precursor in ethanol solution were hydrolyzed under vigorous stirring with distilled H_2O containing HCl used as a catalyst. Then the Al^{3+} and Ni^{3+} ions were introduced in the sol gel process, by dissolving ($\text{Al}(\text{NO}_3)_3 \cdot 9\text{H}_2\text{O}$) and $\text{Ni}(\text{NO}_3)_2 \cdot 6\text{H}_2\text{O}$ in distilled H_2O to the preceding precursors to get the desired concentration. These solutions were stirring for 2 h at room temperature. The resultant homogeneous solutions of monolith materials were filled in molds and aged one week in RT and then dried in a drying oven type GFL 71.5, at about 50°C for about 20 days until no shrinkage appears. Samples were clear and green color. Densification of gels were obtained, by calcination in air for 3h at 900°C , in a muffle furnace with heating rate $5^\circ\text{C}/\text{min}$. X-ray diffraction (XRD) patterns of the prepared samples were recorded with an X-ray diffractometer using monochromatized $\text{CuK}_{\alpha 1}$ radiation of wavelength = 1.54056 \AA . Crystallite sizes G were determined from the Scherer's equation ($G = K\lambda / D \cos\theta$), where K is the Scherer constant (0.9), λ : is the wavelength, and D is the full width (in radians) of the peak at half maximum (FWHM) intensity. The value of G was confirmed by using the U-fit program. The morphological features were studied using JEOL transmission electron microscope JEM-1230 (TEM) and scanning electron microscope (SEM). Fourier Transforms Infrared, were used to determine the individual frequencies and their intensities. The modern Fourier Transform infrared instruments are becoming more commonplace. The magnetic properties were measured using a vibrating sample magnetometer (VSM Model Lakeshore).

3. Results and discussion

3.1. X-ray diffraction (XRD)

The X-ray diffraction patterns for pure phosphosilicate gel (80 P_2O_5 : 20 SiO_2) modified with three different concentrations of aluminum ions in the formula ((80-x) P_2O_5 : 20 SiO_2 : (x= 10, 15 & 20) Al_2O_3) and (59 P_2O_5 : 20 SiO_2 : 20 Al_2O_3 : 1 Ni_2O_3) prepared by sol gel method are shown in Figs. (1, 2). The prepared samples are aged for one week at room temperature before drying at

80°C for 3 weeks and calcined at 900°C for 3h in air as in Fig. 1. All the pure and doped phosphosilicate patterns can be indexed to rhombohedra $\text{Si}_5\text{P}_6\text{O}_{25}$ (JCPDS, no.70-2071), tetragonal SiP_2O_7 (JCPDS, no.22-1320) phases corresponding to the formation of phosphosilicate system and hexagonal $\text{Al}_{23}\text{Si}_5\text{P}_{20}\text{O}_{96}$ (JCPDS, no.52-1178) in the relative intensities of the main peaks. Where these phases consists of isolated SiO_4 , SiO_6 and Si_2O_7 units linked by PO_4 groups in the system phosphosilicate system to form SiO_2 : P_2O_5 nanostructures at lower temperature and linked with AlO_4 to form Al_2O_3 : SiO_2 : P_2O_5 [15]. By increasing the Al_2O_3 content in the phosphosilicate matrix the three preceding phases appeared with higher intensities. This suggests that the presence of Al_2O_3 ions in the sol-gel phosphosilicate helps form smaller phosphosilicate and aluminophosphosilicate network. Fig.2 shows the XRD for (59 P_2O_5 : 20 SiO_2 : 20 Al_2O_3 : 1 Ni_2O_3) calcined at 900°C for 3h in air. By increasing the calcination temperature up to 900°C, the crystallinity and phase separation increase.

The crystallite sizes of the pure phosphosilicate and doped with three different concentrations of Al_2O_3 ions were calculated using Scherrer's formula [16, 17]. The crystallite size of the pure phosphosilicate was 31 nm and for doped with three different concentrations of Al_2O_3 ions, was found to be ranging from (34 nm to 38 nm). The crystallite size for aluminophosphosilicate doped 1 Ni_2O_3 was found to be 45 nm.

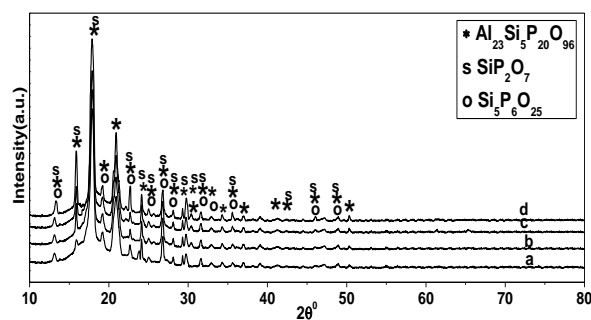


Fig. 1 XRD patterns of (a) phosphosilicate gel and doped with three different concentrations of aluminum ions (b) 10, (c) 15 and (d) 20 mol %, calcined at 900°C for 3h; * $\text{Al}_{23}\text{Si}_5\text{P}_{20}\text{O}_{96}$ phase, o $\text{Si}_5\text{P}_6\text{O}_{25}$ phase and s SiP_2O_7 phase.

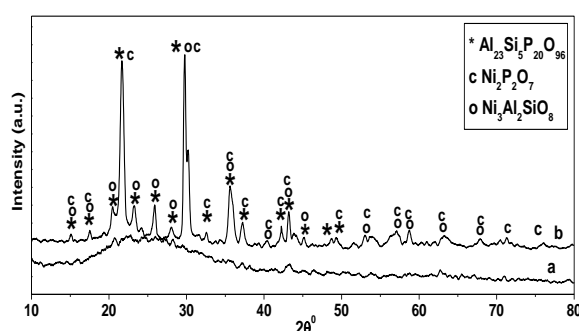


Fig. 2 XRD patterns of monolithic (59 P_2O_5 : 20 SiO_2 : 20 Al_2O_3 : 1 Ni_2O_3) calcined at (a) 300°C and (b) 900°C for 3h in air, * $\text{Al}_{23}\text{Si}_5\text{P}_{20}\text{O}_{96}$ phase, c $\text{Ni}_2\text{P}_2\text{O}_7$ phase and o $\text{Ni}_3\text{Al}_2\text{SiO}_8$ phase.

3.2. Transmission and scanning electron microscopy (TEM/SEM)

Fig. 3 (a, b) shows transmission electron microscopy (TEM) for monolithic phosphosilicate (80 P_2O_5 : 20 SiO_2) doped with two different concentration of Al_2O_3 ions (10 & 20 mol %), calcined at 900°C for 3h in air. It revealed that the distribution of nanoparticles is uniform in the micrograph. The average particle size was found to be 35 nm. Fig. 3 (c, d) shows a SEM

image for the same samples, calcined at 900°C and magnifications of (2000x). As can be seen, some irregularly tiny and fine particles with large aggregates are observable in the micrograph confirms the nano-structure nature for the prepared samples with a high surface/volume ratio. These aggregates consist of numerous spherical phosphosilicate and aluminophosphosilicate crystallites.

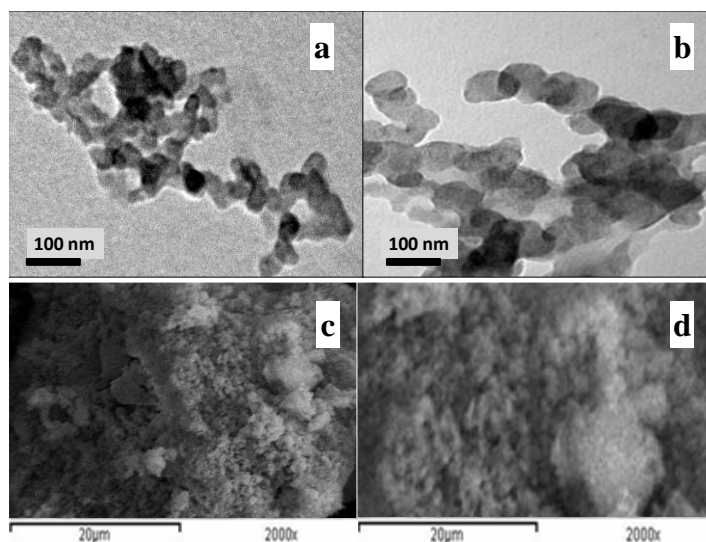


Fig. 3 TEM images of monolithic phosphosilicate doped with (a) 10 and (b) 20 mol% Al_2O_3 ions, and (c, d) SEM images for the same samples, calcined at 900°C for 3h in air.

3.3. FTIR Spectra of monolithic aluminophosphosilicate and doped with Ni_2O_3 ions

Structural properties of monolithic phosphosilicate ($80 \text{ P}_2\text{O}_5: 20 \text{ SiO}_2$) modified with three different concentrations of Al_2O_3 (10, 15, 20 mol %) and ($59 \text{ P}_2\text{O}_5: 20 \text{ SiO}_2: 20 \text{ Al}_2\text{O}_3: 1 \text{ Ni}_2\text{O}_3$) were examined with FTIR spectroscopy. Figs. (4, 5) show the FTIR spectra for the prepared samples in a wide spectral region ($400\text{--}4000 \text{ cm}^{-1}$). The broad absorption band at nearly $3440\text{--}3460 \text{ cm}^{-1}$ assigned to the stretching modes of OH groups, which observed in phosphate-based systems [18-21]. The absorption band at around 1635 cm^{-1} is due to the deformation modes of δ (H–O–H), attributed to bending vibration of crystalline water as interstitial molecules, which could come from KBr in the pellets and the adsorbed water [22, 23]. The shoulder at $1220\text{--}1225 \text{ cm}^{-1}$ may be attributed to P–O and/or P=O stretching vibration, because these bands occur in the fingerprint region ($1320\text{--}1200 \text{ cm}^{-1}$), they cannot be used without some other indication that P is present, because C–O and O–H groups can also absorb strongly in these ranges [21, 22]. By increasing the Al_2O_3 ions in phosphosilicate the intense of the shoulder at 1221 decrease with increasing Al_2O_3 content in the matrix this may be due to the formation of the stretching vibration of the Si–O–Si, Si–O–P and P–O–Al bonds [24, 25]. The band located at 1090 cm^{-1} is attributed to the vibration of P–O–Al, Si–O–Al and P–O–Al–O–Ni bands for the nano-structure aluminophosphosilicate [26, 27]. Silica may exist inside the phosphorus clusters or at the interfaces between P_2O_5 clusters and the SiO_2 matrix in the form of P clusters or P–O–Si bonds, beside the Si–O–Al and P–O–Al bands distributed in the phosphosilicate matrix [26, 27]. The vibration at 962 cm^{-1} and 803 cm^{-1} can be due to stretching vibrations of terminal P–O–, Si–O– and Si–O–P surrounded by P cation in pure phosphosilicate system or corresponding to Si–O–Al, P–O–Al, P–O–Ni and single or double bonds of P–O in the $[\text{PO}_4]^{3-}$ group in aluminophosphosilicate matrix absorbed on the phosphosilicate surface, respectively [28, 29]. The absorption bands in the range from 1100 cm^{-1} to 466 cm^{-1} is associated with phosphate and silica tetrahedral vibrations [6, 14]. The intense of these absorption bands at indicating the formation of well-crystallized nano-sized aluminophosphosilicate and doped with Ni_2O_3 .

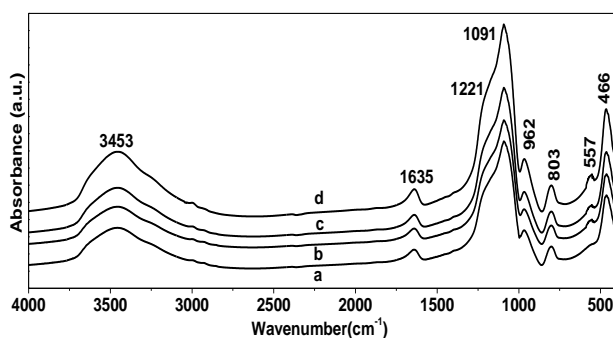


Fig.4 FTIR absorbance spectra of monolithic phosphosilicate (a) and doped with three different concentrations of Al_2O_3 ions (b) 10, (c) 15 and (d) 20 mol %.

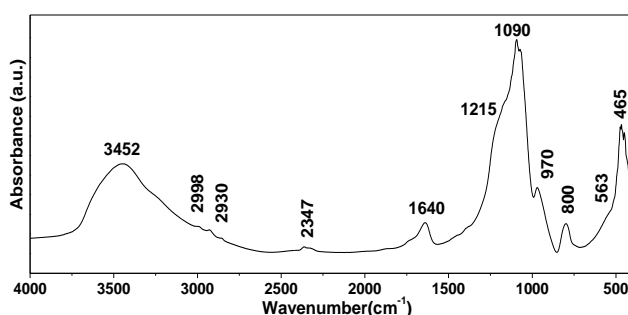


Fig. 5 XRD patterns of monolithic (60 P_2O_5 : 20 SiO_2 : 20 Al_2O_3 : 1 Ni_2O_3) calcined at $200^\circ C$ for 3h in air.

3. 4. The magnetic Analysis

Magnetic properties are measured by a vibrating sample magnetometer. The magnetic hysteresis loop at room temperature of monolithic aluminophosphosilicate doped with 1 mol% of Ni_2O_3 ions as in the formula (59 P_2O_5 : 20 SiO_2 : 20 Al_2O_3 : 1 Ni_2O_3), calcined at $900^\circ C$ for 3h in air is shown in Fig. 6. The corresponding magnetic parameters for the prepared sample are reported in Table 1. Where, the movement of magnetic domain (Ni_2O_3) is the main reason for coercivity. Here, the surface domain (Ni_2O_3) should be present covalently bonded and/or the interface between (Ni_2O_3) and the aluminophosphosilicate matrix. These results indicate that the prepared sample using the sol gel method have low magnetic properties according to the glasses nature for the phosphosilicate-based nanostructures.

Table(1): Magnetic parameters of aluminophosphosilicate doped with 1 mol% Ni_2O_3 ions

Sample name	M_s (emu)	M_r (emu/g)	H_c (G)	Squareness (M_r/M_s)
59 P_2O_5 : 20 SiO_2 : 20 Al_2O_3 : 1 Ni_2O_3	26.631×10^{-3}	24.400×10^{-3}	156.40	91.625

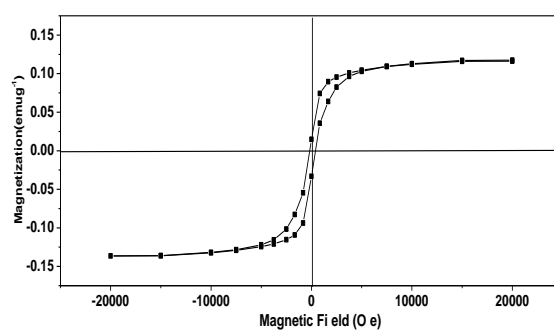


Fig. 6 The M-H curves (hysteresis loop) recorded at room temperature for (a) 59 P₂O₅: 20 SiO₂: 20 Al₂O₃: 1 Ni₂O₃.

4. Conclusions

Homogeneous nanostructure ((60-x) P₂O₅: 20 SiO₂: (x=10,15, 20) Al₂O₃) and doped with 1 mol % Ni₂O₃ were prepared by sol gel method and calcined at 900°C. Structural studies by XRD, TEM and FTIR spectroscopy revealed the incorporation of Al₂O₃ ions with high concentrations serve to polymerize the phosphosilicate glasses, resulting in both the increased chemical stability and the crystallinity. The FTIR results indicate that nonbridging oxygens are linked to hydrogens from phosphanol (P–OH), silanol moieties (Si–OH) and (Al–OH). The incorporation of Al₂O₃ units into the phosphosilicate structural network results in the depolymerisation of phosphate chains in phosphosilicate network. Besides the formation of P–O–Al bonds, also the formation of P–O–Si–O–Al bonds. The magnetic result for the (59 P₂O₅: 20 SiO₂: 20 Al₂O₃: 1 Ni₂O₃) indicate that the prepared samples have low magnetic properties according to the glasses nature for the phosphosilicate-based nanostructures.

References

- [1] R. Murugavel, A. Choudhury, M.G. Walawalkar, R. Pothiraja, C.N.R. Rao, Chem. Rev. **108**, 3549 (2008).
- [2] Ar. G. Kannan, N. R. Choudhury, N. K. Dutta, J of Electroanalytical Chemi., **641**, 28 (2010).
- [3] R. Catteaux, I. G-Lebecq, F. Désanglois, F. Chai, J-C. Hornez, S. Hampshire, C. F-Houttemane, Chemi. Engine. Research and Design, **91**, 2420 (2013).
- [4] V. Raj, M. S. Mumjitha, Electrochimica Acta **153**, 1 (2015).
- [5] E. Metwalli, M. Karabulut, L. D.Sidebottom, M. M. Morsi, K. R. Brow, J Non-Cryst Solids **344**, 128 (2004)–134.
- [6] A. M. Elnahrawy, A. Ibrahim, New J. of Glass and Ceram., **4**, 42 (2014).
- [7] A. Ananthanarayanan, G.P.Kothiyal, L.Montagne, B.Revel, J of Solid State Chem., **183**, 1416 (2010).
- [8] P.Riello, P. Canton, N. Comelato, S.Polizi, M. Verit, G. Fagherazzi, H. Hofmeister, S.Hopfe, J.Non-Cryst.Solids, **288**, 127 (2001).
- [9] G. A. Khater, M. H. Idris, Ceram.Int.**33**, 233 (2007).
- [10] K. Zheng, S. Yang, J. Wang, C.Rüssel, C. Liu, W. Liang, J of Non-Crystalline Solids **358**, 387 (2012).
- [11] C.J. Brinker and G.W. Scherer, Sol–Gel Science: The Physics and Chemistry of Sol–Gel Processing, Academic Press, New York (1990).
- [12] N.H. Ray, Inorganic Polymers, Academic Press, London, 1978 pp. 79–90.
- [13] A. M Elnahrawy, IJAETCS, **2**, 15 (2015).
- [14] A. M. Elnahrawy, Y. S. Kim, A. I. Ali, Jof Alloys and Compounds **676**, 432 (2016).
- [15] J. Perez-Pariente, F. Balas, J. Roman, A.J. Salinas, M. Vallet-Reg, J. Biomed. Mater. Res.

- 61**, 524 (2002).
- [16] A.L. Patterson, The Scherrer formula for X-Ray particle size determination, *Phys. Rev* **56**, 978 (1939).
- [17] S.A. Hassanzadeh-Tabrizi, *Trans. Nonferrous Met. Soc. China* **21**, 2443 (2011).
- [18] H. Aguiar, E.L. Solla, J. Serra, P. González, B. León, N. Almeida, S. Cachinho, E.J.C. Davim, R. Correia, J.M. Oliveira, M.H.V. Fernandes, *J of Non-Cryst. Solids*, **354**, 4075 (2008).
- [19] Mohamed M. ElOkr, F. Metawe, Amany M El-Nahrawy, Basma A. A. Osman, *Intern. J of ChemTech Research*, **9**, 228 (2016).
- [20] A. Charkhi, M. Kazemeini, S.J. Ahmadi, H. Kazemian, *Powder Techno.*, **231**, 1 (2012).
- [21] G. Lakshminarayana, M. Nogami, I.V. Kityk, *J of Allo. & Comp.*, **509**, 2238 (2011).
- [22] D. L. Wood, *J. Am. Ceram. Soc.* **66**, 693 (1982).
- [23] Y-H. Han, A. Taylor, M. D. Mantle, K. M. Knowles, *J of Non- Cryst. Solids* **353**, 313 (2007)
- [24] S. Sambandam, V. Ramani, *J. Power Sources* **170**, 259 (2007).
- [25] K. Takeuchi, M. Terano, T. Taniike, *Polymer* **55**, 1940 (2014).
- [26] R. M. Filgueiras, G. LaTorre, L. L. Hench, *J Biomed Mater Res*, **27**, 445 (1993).
- [27] S. Kongwudthiti, P. Praserttham, W. Tanakulrungsank, M. Inoue, *J Mater Process Technol*, **136**, 186 (2003).
- [28] I. Izquier-Barba, A.J. Salinas, M. Vallet-Regí, *Int.J.App. Glas.Sci.* **4**(2), 149 (2013).
- [29] R.L. Siqueira, E.D. Zanotto, *J.Mater.Sci.:Mater.Med.* **24**, 365 (2013).